PHYSICAL REVIEW B VOLUME 22, NUMBER 10 15 NOVEMBER 1980

# Effect of uniaxial stress on the excitonic molecule bound to nitrogen trap in GaP

H. Mathieu, P. Merle, L. Bayo, and J. Camassel
*Centre d'Etudes d'Electronique des Solides* Université des Sciences et Techniques du Languedoc, 34060-Montpellier-Cedex, France*
(Received 30 June 1980)

We have investigated the experimental and theoretical stress dependence of the excitonic molecule bound to the isoelectronic nitrogen trap in GaP. Data have been collected at pumped-liquid-helium temperature for the stress directions [001], [111], and [110] respectively. The quantitative stress dependence is consistent with the identification previously reported by Merz *et al.* concerning the energy states of the complex. $A^*$ and $B^*$ photoluminescence lines result from the radiative recombination of an exciton constituting the excitonic molecule bound at a nitrogen atom. The ground states of the transition are the two $J=1$ and $J=2$ states of the single bound exciton. The intervalley-coupling matrix element $\Delta$ appears to be much smaller for the bound excitonic molecule than for the single bound exciton. We find $\Delta = 2.3$ meV for the bound excitonic molecule compared with $\Delta = 8$ meV for the single bound exciton.

## I. INTRODUCTION

The isoelectronic substitution of N for P in GaP is known to produce many bound-exciton states which have been extensively described in a recent review of bound excitons in semiconductors by Dean and Herbert.[1]

Briefly, for dilute concentration and relatively low excitation, the recombination spectrum exhibits the well-known $A$ and $B$ no-phonon lines associated with the decay of an exciton bound to a single nitrogen atom. These bound-exciton states have been investigated in detail, both experimentally[2-6] and theoretically.[7-9]

For heavier doping, excitons interact not only with a single N site but also with pairs of atoms labeled $NN_i$ in the literature.[2,10,11] The greater the pair separation, the smaller the exciton binding energy. Such highly doped samples exhibit a series of isoelectronic traps which converge to the value for a single isolated nitrogen.

For dilute concentration but relatively high excitation, two additional series of recombination lines appear slighly above the $A$-$B$ manifold characteristic of the single bound exciton. These lines, first observed by Cuthbert and Thomas,[12] were associated with excited states of the bound exciton. Next they were cited by Faulkner[7] and associated with some higher valley-orbit state of the trapped electron in the bound-exciton state. Finally these lines labeled $A^*$ and $B^*$ were investigated in detail by Merz *et al.*[13] and identified as the recombination of a "bound excitonic molecule." The initial state is the bound excitonic molecule and the final state is a single bound exciton. The purpose of this paper is to study the uniaxial stress dependence of the $A^*$ and $B^*$ lines, and thereby substantiate the proposed model.

## II. THEORY

### A. Basis states

#### *1. Bound exciton*

The ground state of the bound exciton (BE) is made of an electron localized in the $\Gamma_6$ valley-orbit split state and a hole associated with the $\Gamma_8$ valence-band maximum. The $j$-$j$ interaction between the electron and the hole gives rise to a $J=1$ triplet of energy $E_0+5\gamma/8$ and a $J=2$ quintet of energy $E_0-3\gamma/8$. The exchange energy $\gamma$ depends upon the electron-hole overlap. The effect of the crystal field is expected to induce mixing of the exciton basis states and hence a splitting of the $J=2$ state into a $\Gamma_{12}$ doublet and a $\Gamma_{15}$ triplet. However, as discussed by Onton and Morgan,[14] since each basis state is formed from a combination of one $p$-like and one $s$-like state, there will be no mixing by the spin-independent $T_d$ crystal field and the crystal-field splitting is expected to be vanishingly small. Indeed it has never been observed. As a consequence, the zero-stress basis states of the bound exciton can be taken as eigenfunctions of the angular momenta $J=1$ and $J=2$ and symbolized by a ket $|JM\rangle$. They are built up of linear combinations of functions $|j_h, m_h; j_e, m_e\rangle$ hereafter labeled $|m_h, m_e\rangle$. The coefficients of the different combinations are the Clebsh-Gordan coefficients and the basis functions are the following:

$J=1$:

$$|1,\pm1\rangle = \mp\tfrac{1}{2}\left(\left|\pm\tfrac{1}{2},\pm\tfrac{1}{2}\right\rangle \pm\sqrt{3}\left|\pm\tfrac{3}{2},\mp\tfrac{1}{2}\right\rangle\right),$$
$$|1,0\rangle = -\tfrac{1}{2}\sqrt{2}\left(\left|-\tfrac{1}{2},\tfrac{1}{2}\right\rangle + \left|\tfrac{1}{2},-\tfrac{1}{2}\right\rangle\right), \quad (1a)$$

 

$J=2$:

$$|2,\pm2\rangle = |\pm\tfrac{3}{2},\pm\tfrac{1}{2}\rangle ,$$
$$|2,\pm1\rangle = \tfrac{1}{2}(\sqrt{3}\,|\pm\tfrac{1}{2},\pm\tfrac{1}{2}\rangle + |\pm\tfrac{3}{2}\mp\tfrac{1}{2}\rangle) , \quad (1b)$$
$$|2,0\rangle = \tfrac{1}{2}\sqrt{2}(|-\tfrac{1}{2},\tfrac{1}{2}\rangle + |\tfrac{1}{2},-\tfrac{1}{2}\rangle) .$$

### 2. Bound excitonic molecule

The ground state of the bound excitonic molecule (BEM) consists[13] of two electrons with spin $S=\frac{1}{2}$ in the $\Gamma_6$ valley-orbit split state and two holes with angular momentum $J=\frac{3}{2}$ associated with the $\Gamma_8$ valence-band maximum. The electrons only couple with antiparallel spins and contribute no net angular momentum. On account of the Pauli principle, the vector coupling of the $J=\frac{3}{2}$ angular momenta of the holes results in two antisymmetric states: $J=0$ of energy $E_0'+\frac{5}{8}\delta$ and $J=2$ of energy $E_0'-\frac{3}{8}\delta$. The exchange energy $\delta$ depends upon the hole-hole overlap, and the resulting states are built of linear combinations of functions $|j_{h1},m_{h1};j_{h2},m_{h2};j_{e1},m_{e1};j_{e2},m_{e2}\rangle$ hereafter labeled $|m_{h1},m_{h2}\rangle$.

The basis functions are the following:

$J=0$:

$$|0,0\rangle = \frac{1}{\sqrt{2}}(|-\tfrac{3}{2},\tfrac{3}{2}\rangle + |-\tfrac{1}{2},\tfrac{1}{2}\rangle), \quad (2a)$$

$J=2$:

$$|2,\pm2\rangle = |\pm\tfrac{3}{2},\pm\tfrac{1}{2}\rangle ,$$
$$|2,\pm1\rangle = |\pm\tfrac{3}{2},\mp\tfrac{1}{2}\rangle , \quad (2b)$$
$$|2,0\rangle = \frac{1}{\sqrt{2}}(-|-\tfrac{3}{2},\tfrac{3}{2}\rangle + |-\tfrac{1}{2},\tfrac{1}{2}\rangle) .$$

The crystal field splits the $J=2$ state into a $\Gamma_{12}$ doublet of energy $E_0'-\frac{3}{8}\delta+\frac{2}{5}\beta$ and a $\Gamma_{25}$ triplet of energy $E_0'-\frac{3}{8}\delta-\frac{3}{5}\beta$. $\beta$ is the crystal-field splitting energy. The coupled states are formed from a combination of two $p$-like states, and, contrary to the case of the single bound exciton, the crystal-field splitting is expected to be nonzero. It has been observed.[13] As a consequence the zero-stress basis state on the bound excitonic molecule will be taken as the $|\Gamma_1\rangle$, $|\Gamma_{12}\rangle$, and $|\Gamma_{25}\rangle$ states. They are given as a function of the $|m_{h1},m_{h2}\rangle$ states quantized along the [001] crystallographic direction by

$\Gamma_1$:

$$|\Gamma_1\rangle = \frac{1}{\sqrt{2}}(|-\tfrac{3}{2},\tfrac{3}{2}\rangle + |-\tfrac{1}{2},\tfrac{1}{2}\rangle) , \quad (3a)$$

$\Gamma_{25}$:

$$|\Gamma_{25}^{xy}\rangle = \frac{i}{\sqrt{2}}(-|\tfrac{3}{2},\tfrac{1}{2}\rangle + |-\tfrac{3}{2},-\tfrac{1}{2}\rangle) ,$$
$$|\Gamma_{25}^{xz}\rangle = \frac{1}{\sqrt{2}}(|\tfrac{3}{2},-\tfrac{1}{2}\rangle + |-\tfrac{3}{2},\tfrac{1}{2}\rangle) , \quad (3b)$$
$$|\Gamma_{25}^{yz}\rangle = \frac{i}{\sqrt{2}}(-|\tfrac{3}{2},-\tfrac{1}{2}\rangle + |-\tfrac{3}{2},\tfrac{1}{2}\rangle) ,$$

$\Gamma_{12}$:

$$|\Gamma_{12}^{a}\rangle = \frac{1}{\sqrt{2}}(|\tfrac{3}{2},\tfrac{1}{2}\rangle + |-\tfrac{3}{2},-\tfrac{1}{2}\rangle) ,$$
$$|\Gamma_{12}^{b}\rangle = \frac{1}{\sqrt{2}}(-|-\tfrac{3}{2},\tfrac{3}{2}\rangle + |-\tfrac{1}{2},\tfrac{1}{2}\rangle) . \quad (3c)$$

### 3. Transition lines

The transitions from the $J=1$ and $J=2$ BE states to the $J=0$ crystal ground state lead to the $A$ line (dipole allowed) and $B$ line (dipole forbidden), respectively.

The transitions from the BEM states to the $J=1$ and $J=2$ BE states lead to the $A^*$ and $B^*$ sets of lines, respectively. In other words the lines $A^*$ and $B^*$ result from the radiative recombination of one of the two excitons which form the bound excitonic molecule, leaving a single exciton bound to nitrogen. The initial states of the transitions are the $J=0$ and $J=2$ (split into $\Gamma_{12}$ and $\Gamma_{25}$ levels) states of the BEM. The final states are the $J=1$ and $J=2$ levels of the BE. Transitions from the $J=0$ and $J=2$ BEM states to the $J=1$ BE state are dipole allowed ($\Delta J=\pm1$) and give rise to the three components of the $A^*$ line. However, transitions to the $J=2$ BE state are only allowed from the $J=2$ BEM state and give rise to the two components of the $B^*$ line. The BE states, BEM states, $A$-$B$ lines, and $A^*$-$B^*$ sets of lines are summarized in Fig. 1, where the full lines represent dipole-allowed transitions and the broken lines represent dipole-forbidden transitions.

## B. Stress dependence

The stress dependence of the $|m_i,m_j\rangle$ zero-order states ($|m_h,m_e\rangle$ for the BE, $|m_{h1},m_{h2}\rangle$ for the BEM) is obtained by just adding the stress dependence of the constitutive particles and, of course, in the $|m_i,m_j\rangle$ basis is described by diagonal terms. These terms include:

(i) the hydrostatic component. It corresponds for each exciton to the expression

$$A_i = a_i(S_{11}+2S_{12})X ,$$

where $a_i$ is the hydrostatic deformation potential of a given bound exciton and $S_{ij}$ are the elastic compliance constants. $X$ is the stress magnitude and is taken to be negative for a compression. Index $i=1$ refers to the BE and $i=2$ to an exciton of the BEM.

(ii) The shear-strain dependence of the bound electron(s). It reflects the change in degeneracy of the three [001] minima of the conduction band. This component which has been calculated for the BE in the valley repopulation model,[6] is given by expressions like

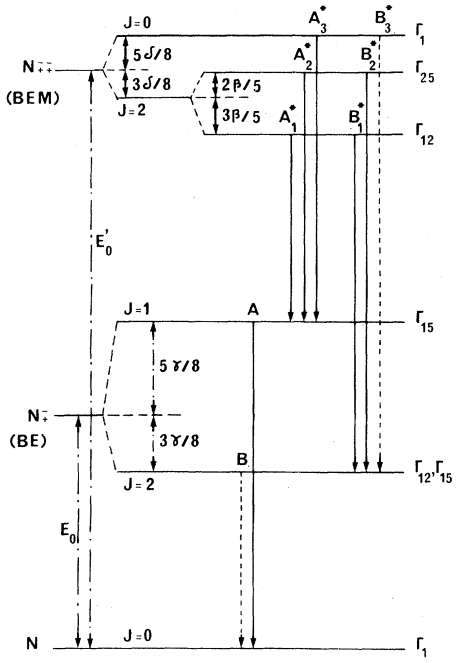


FIG. 1. Energy-level diagram of the bound excitonic molecule ($N^{++}$), of the bound exciton ($N^{+}$) and of the crystal ground state (N). The transition lines are labeled in agreement with Ref. 13. The full lines represent dipole-allowed transitions. The broken lines represent the dipole-forbidden transitions. $\gamma$ is the electron-hole exchange energy, $\delta$ is the hole-hole exchange energy and $\beta$ represents the crystal-field splitting.

$$E(\Gamma_1)_i = \tfrac{1}{2}\Delta_i[-1 + x - 3(1 + \tfrac{2}{3}x + x^2)^{1/2}], \qquad (4)$$

where $x = E_2 S/6\Delta_i$ and $S = 2(S_{11} - S_{12})X$, $-(S_{11} - S_{12})X$, and 0 for $\vec{X}\|[001]$, [110], and [111], respectively.

Again $i = 1$ refers to the BE and $i = 2$ to an electron of the BEM. $\Delta_i$ is the intervalley-coupling matrix element and $E_2$ is the shear deformation potential of the $X_1$ valleys.[6,15]

(iii) The shear-strain dependence of the bound hole(s). It is directly related to the splitting of the $\Gamma_8$ valence band and has been recently measured for the BE.[6] It has been found isotropic and equal to the splitting of the free exciton. Since, on the other hand, the stress dependence of the BEM has been observed only under very low stress conditions (typically up to 400 bars; see Figs. 5, 6 and 7), in these conditions the stress-induced coupling between the $\Gamma_8$ valence band and the $\Gamma_7$ spin-orbit split-off valence band,[15] can be ignored. In other words the splitting of the bound hole(s) will be simply given by $\pm\epsilon$ with $\epsilon = (d/2\sqrt{3})S_{44}X = b\,(S_{11} - S_{12})X$. $d$ and $b$ are the well-known shear deformation potentials of the $\Gamma_8$ valence band.[15] The splitting of the $|m_i, m_j\rangle$ zero-order states are then given by

BE:

$$\Delta E = \begin{cases} +\epsilon & \text{for the } |\pm\tfrac{3}{2}, m_e\rangle \text{ states}, \\ -\epsilon & \text{for the } |\pm\tfrac{1}{2}, m_e\rangle \text{ states}, \end{cases} \qquad (5)$$

BEM:

$$\Delta E = \begin{cases} +2\epsilon & \text{for the } |\pm\tfrac{3}{2}, \mp\tfrac{3}{2}\rangle \text{ states}, \\ 0 & \text{for the } |\pm\tfrac{3}{2}, \pm\tfrac{1}{2}\rangle \text{ and } |\pm\tfrac{3}{2}, \mp\tfrac{1}{2}\rangle \text{ states}, \\ -2\epsilon & \text{for the } |\pm\tfrac{1}{2}, \mp\tfrac{1}{2}\rangle \text{ states}. \end{cases} \qquad (6)$$

### *1. Bound exciton*

Now, on the basis of the $J = 1$ and $J = 2$ states which diagonalize the BE states at zero stress [Eqs. (1)], the strain-matrix becomes

$$\begin{array}{c} |10\rangle \quad |1\pm1\rangle \quad |2\pm1\rangle \quad |2\pm2\rangle \quad |20\rangle \\ \begin{pmatrix} E_1 + \frac{5}{8}\gamma - \epsilon & 0 & 0 & 0 & 0 \\ 0 & E_1 + \frac{5}{8}\gamma + \frac{1}{2}\epsilon & \pm\frac{1}{2}\sqrt{3}\,\epsilon & 0 & 0 \\ 0 & \pm\frac{1}{2}\sqrt{3}\,\epsilon & E_1 - \frac{3}{8}\gamma - \frac{1}{2}\epsilon & 0 & 0 \\ 0 & 0 & 0 & E_1 - \frac{3}{8}\gamma + \epsilon & 0 \\ 0 & 0 & 0 & 0 & E_1 - \frac{3}{8}\gamma - \epsilon \end{pmatrix} \end{array}, \qquad (7)$$

where $E_1 = E_0 + A_1 + E(\Gamma_1)_1$.

The stress dependence of the BE states are then given by

$J = 1$:

$$W_1^1 = E_1 + \tfrac{5}{8}\gamma - \epsilon, \qquad (8a)$$

$$W_1^2 = E_1 + \tfrac{1}{8}\gamma + (\tfrac{1}{4}\gamma^2 + \tfrac{1}{2}\gamma\epsilon + \epsilon^2)^{1/2}, \qquad (8b)$$

$J=2$:

$$W_1^3 = E_1 + \tfrac{1}{8}\gamma - (\tfrac{1}{4}\gamma^2 + \tfrac{1}{2}\gamma\epsilon + \epsilon^2)^{1/2}, \tag{8c}$$

$$W_1^4 = E_1 - \tfrac{3}{8}\gamma + \epsilon, \tag{8d}$$

$$W_1^5 = E_1 - \tfrac{3}{8}\gamma - \epsilon. \tag{8e}$$

### 2. Bound excitonic molecule

Again on the basis of the $|\Gamma_1\rangle$, $|\Gamma_{12}\rangle$, and $|\Gamma_{25}\rangle$ states which diagonalize the BEM states at zero stress [Eqs. (3)], the strain matrix becomes

$$\begin{array}{c} \begin{array}{cccccc} |\Gamma_1\rangle & |\Gamma_{25}^{xy}\rangle & |\Gamma_{25}^{xz}\rangle & |\Gamma_{25}^{yz}\rangle & |\Gamma_{12}^{a}\rangle & |\Gamma_{12}^{b}\rangle \end{array} \\ \begin{pmatrix} E_2+\frac{5}{8}\delta & p & q & q & 0 & r \\ p & E_2-\frac{3}{8}\delta+\frac{2}{5}\beta & 0 & 0 & 0 & 0 \\ q & 0 & E_2-\frac{3}{8}\delta+\frac{2}{5}\beta & 0 & 0 & 0 \\ q & 0 & 0 & E_2-\frac{3}{8}\delta+\frac{2}{5}\beta & 0 & 0 \\ 0 & 0 & 0 & 0 & E_2-\frac{3}{8}\delta-\frac{3}{5}\beta & 0 \\ r & 0 & 0 & 0 & 0 & E_2-\frac{3}{8}\delta-\frac{3}{5}\beta \end{pmatrix} \end{array}, \tag{9}$$

where

$$E_2 = E_0' + 2A_2 + 2E(\Gamma_1)_2,$$

and for

$\vec{X}||[001]$ $p=q=0$, $r=2\epsilon$

$\vec{X}||[111]$ $p=q=(2/\sqrt{3})\epsilon$, $r=0$

$\vec{X}||[110]$ $p=\sqrt{3}\,\epsilon$, $q=0$, $r=-\epsilon$.

For $\vec{X}||[001]$ or [111] all energy eigenvalues can be obtained analytically while, for $\vec{X}||[110]$, the matrix equation (9) must be solved numerically. The stress dependence of the various BEM states are then given by

$\vec{X}||[001]$:

$$W_2^1 = E_2 + \tfrac{1}{8}\delta - \tfrac{3}{10}\beta + [\tfrac{1}{4}(\delta + \tfrac{3}{5}\beta)^2 + 4\epsilon^2]^{1/2}, \tag{10a}$$

$$W_2^2 = E_2 - \tfrac{3}{8}\delta + \tfrac{2}{5}\beta, \tag{10b}$$

$$W_2^3 = E_2 - \tfrac{3}{8}\delta - \tfrac{3}{5}\beta, \tag{10c}$$

$$W_2^4 = E_2 + \tfrac{1}{8}\delta - \tfrac{3}{10}\beta - [\tfrac{1}{4}(\delta + \tfrac{3}{5}\beta)^2 + 4\epsilon^2]^{1/2}. \tag{10d}$$

The state of energy $W_2^2$ remains threefold degenerate,

$\vec{X}||[111]$:

$$W_2^1 = E_2 + \tfrac{1}{8}\delta + \tfrac{1}{5}\beta + [\tfrac{1}{4}(\delta - \tfrac{2}{5}\beta)^2 + 4\epsilon^2]^{1/2}, \tag{11a}$$

$$W_2^2 = E_2 + \tfrac{1}{8}\delta + \tfrac{1}{5}\beta - [\tfrac{1}{4}(\delta - \tfrac{2}{5}\beta)^2 + 4\epsilon^2]^{1/2}, \tag{11b}$$

$$W_2^3 = E_2 - \tfrac{3}{8}\delta + \tfrac{2}{5}\beta, \tag{11c}$$

$$W_2^4 = E_2 - \tfrac{3}{8}\delta - \tfrac{3}{5}\beta. \tag{11d}$$

The states of energies $W_2^3$ and $W_2^4$ are twofold degenerate;

$\vec{X}||[110]$:

$$W_2^1 = E_2 + V_1, \tag{12a}$$

$$W_2^2 = E_2 + V_2, \tag{12b}$$

$$W_2^3 = E_2 - \tfrac{3}{8}\delta + \tfrac{2}{5}\beta, \tag{12c}$$

$$W_2^4 = E_2 - \tfrac{3}{8}\delta - \tfrac{3}{5}\beta, \tag{12d}$$

$$W_2^5 = E_2 + V_3, \tag{12e}$$

where $V_1$, $V_2$, and $V_3$ are the eigenvalues of the $3\times3$ matrix: $|\Gamma_1\rangle$; $|\Gamma_{25}^{xy}\rangle$; $|\Gamma_{12}^{b}\rangle$. The state of energy $W_2^3$ is twofold degenerate.

### 3. Transition lines

All stress dependences and selection rules of the transition lines are given in Table I. We notice that the $B_3^*$ component which is dipole forbidden at zero stress becomes stress allowed in $\sigma$ polarization. On the other hand, it should be noted that the $B_1^*$ ($A_1^*$) component splits into six (four) subcomponents under [001] stress and only three (two) subcomponents under [111] stress. It is the reverse for the $B_2^*$ ($A_2^*$) component. This corresponds to the fact that the $B_1^*$ ($A_1^*$) component is associated with the $\Gamma_{12}$ BEM state which splits under [001] stress but remains degenerate under [111] stress. The reverse is true for the $B_2^*$ ($A_2^*$) component which is associated with the $\Gamma_{25}$ BEM state. For a [110] stress both $\Gamma_{12}$ and $\Gamma_{25}$ are stress split so that $B_1^*$ ($A_1^*$) and $B_2^*$ ($A_2^*$) give rise to six (four) subcomponents. All results for the [001] stress direction are summarized in Fig. 2,

TABLE I. Stress dependences and selection rules of the transition lines. The stress dependences of the final states $W_1^i$ are given by Eqs. (8). The stress dependences of the initial states $W_2^j$ are given by Eqs. (10), (11), and (12) for $\vec{X} \| [001]$, [111], and [110], respectively. $\sigma$ polarization corresponds to $\vec{E} \perp \vec{X}$, $\pi$ polarization corresponds to $\vec{E} \| \vec{X}$, 0 corresponds to dipole-forbidden transition. The $B_3^*$ component is zero-stress forbidden and the $B_3^{*2}$ subcomponent is stress allowed.

| Zero-stress lines | | | Stress direction $\vec{X} \| [001]$ | | $\vec{X} \| [111]$ | | $\vec{X} \| [110]$ | |
|---|---|---|---|---|---|---|---|---|
| $B^*$ | $B_3^*$ | $B_3^{*3}$ | $W_2^1 - W_1^5$ | 0 | $W_2^1 - W_1^5$ | 0 | $W_2^1 - W_1^5$ | 0 |
| | | $B_3^{*2}$ | $W_2^1 - W_1^3$ | $\sigma$ | $W_2^1 - W_1^3$ | $\sigma$ | $W_2^1 - W_1^3$ | $\sigma$ |
| | | $B_3^{*1}$ | $W_2^1 - W_1^4$ | 0 | $W_2^1 - W_1^4$ | 0 | $W_2^1 - W_1^4$ | 0 |
| | $B_2^*$ | $B_2^{*6}$ | | | $W_2^3 - W_1^5$ | $\sigma$ | $W_2^3 - W_1^5$ | $\sigma$ |
| | | $B_2^{*5}$ | | | $W_2^3 - W_1^3$ | $\pi\sigma$ | $W_2^3 - W_1^3$ | $\pi\sigma$ |
| | | $B_2^{*4}$ | | | $W_2^3 - W_2^4$ | $\pi\sigma$ | $W_2^3 - W_1^4$ | $\pi\sigma$ |
| | | $B_2^{*3}$ | $W_2^2 - W_1^5$ | $\sigma$ | $W_2^2 - W_1^5$ | 0 | $W_2^5 - W_1^5$ | 0 |
| | | $B_2^{*2}$ | $W_2^2 - W_1^3$ | $\pi\sigma$ | $W_2^2 - W_1^3$ | $\sigma$ | $W_2^5 - W_1^3$ | $\sigma$ |
| | | $B_2^{*1}$ | $W_2^2 - W_1^4$ | $\pi\sigma$ | $W_2^2 - W_1^4$ | 0 | $W_2^5 - W_1^4$ | 0 |
| | $B_1^*$ | $B_1^{*6}$ | $W_2^3 - W_1^5$ | 0 | | | $W_2^4 - W_1^5$ | $\sigma$ |
| | | $B_1^{*5}$ | $W_2^3 - W_1^3$ | $\sigma$ | | | $W_2^4 - W_1^3$ | $\pi\sigma$ |
| | | $B_1^{*4}$ | $W_2^3 - W_1^4$ | $\pi$ | | | $W_2^4 - W_1^4$ | $\pi\sigma$ |
| | | $B_1^{*3}$ | $W_2^4 - W_1^5$ | 0 | $W_2^4 - W_1^5$ | $\sigma$ | $W_2^2 - W_1^5$ | 0 |
| | | $B_1^{*2}$ | $W_2^4 - W_1^3$ | $\sigma$ | $W_2^4 - W_1^3$ | $\pi\sigma$ | $W_2^2 - W_1^3$ | $\sigma$ |
| | | $B_1^{*1}$ | $W_2^4 - W_1^4$ | 0 | $W_2^4 - W_1^4$ | $\pi\sigma$ | $W_2^2 - W_1^4$ | 0 |
| $A^*$ | $A_3^*$ | $A_3^{*2}$ | $W_2^1 - W_1^1$ | $\pi$ | $W_2^1 - W_1^1$ | $\pi$ | $W_2^1 - W_1^1$ | $\pi$ |
| | | $A_3^{*1}$ | $W_2^1 - W_1^2$ | $\sigma$ | $W_2^1 - W_1^2$ | $\sigma$ | $W_2^1 - W_1^2$ | $\sigma$ |
| | $A_2^*$ | $A_2^{*4}$ | | | $W_2^3 - W_1^1$ | $\sigma$ | $W_2^3 - W_1^1$ | $\sigma$ |
| | | $A_2^{*3}$ | | | $W_2^3 - W_1^2$ | $\pi\sigma$ | $W_2^3 - W_1^2$ | $\pi\sigma$ |
| | | $A_2^{*2}$ | $W_2^2 - W_1^1$ | $\sigma$ | $W_2^2 - W_1^1$ | $\pi$ | $W_2^5 - W_1^1$ | $\pi$ |
| | | $A_2^{*1}$ | $W_2^2 - W_1^2$ | $\pi\sigma$ | $W_2^2 - W_1^2$ | $\sigma$ | $W_2^5 - W_1^2$ | $\sigma$ |
| | $A_1^*$ | $A_1^{*4}$ | $W_2^3 - W_1^1$ | 0 | | | $W_2^4 - W_1^1$ | $\sigma$ |
| | | $A_1^{*3}$ | $W_2^3 - W_1^2$ | $\sigma$ | | | $W_2^4 - W_1^2$ | $\pi\sigma$ |
| | | $A_1^{*2}$ | $W_2^4 - W_1^1$ | $\pi$ | $W_2^4 - W_1^1$ | $\sigma$ | $W_2^2 - W_1^1$ | $\pi$ |
| | | $A_1^{*1}$ | $W_2^4 - W_1^2$ | $\sigma$ | $W_2^4 - W_1^2$ | $\pi\sigma$ | $W_2^2 - W_1^2$ | $\sigma$ |

where the dipole-allowed transitions are indicated by arrows.

## III. EXPERIMENTAL RESULTS AND DISCUSSION

### A. Zero-stress spectrum

Figure 3 shows a typical low-temperature photoluminescence spectrum obtained from a nitrogen-doped gallium phosphide sample excited by the 5145-Å line of an argon laser. This spectrum clearly shows the two lines $A$-$B$ associated with the recombination of a single bound exciton. At low temperature the low-energy $J=2$ BE state is much more populated than the high-energy $J=1$ state so that the forbidden transition from the $J=2$ BE state ($B$ line) is clearly observed. The $A^*$ and $B^*$ sets of lines appear on the high-energy side of the spectrum but at least are one order of magnitude smaller. In agreement with the theoretical model, the $B_3^*$ component is forbidden. From the energy of these spectral lines, we deduce three parameters of the theoretical model used in Sec. II. Averaging a series of measurements obtained on different samples, we find $\gamma = 0.90$ meV, $\delta = 0.18$ meV, and $\beta = 0.17$ meV. All values are in perfect agreement with those given by Merz *et al.*[13]

Also note the structure which appears on the high-energy side of the $A$ line. This structure, which has never been observed up to data, is not

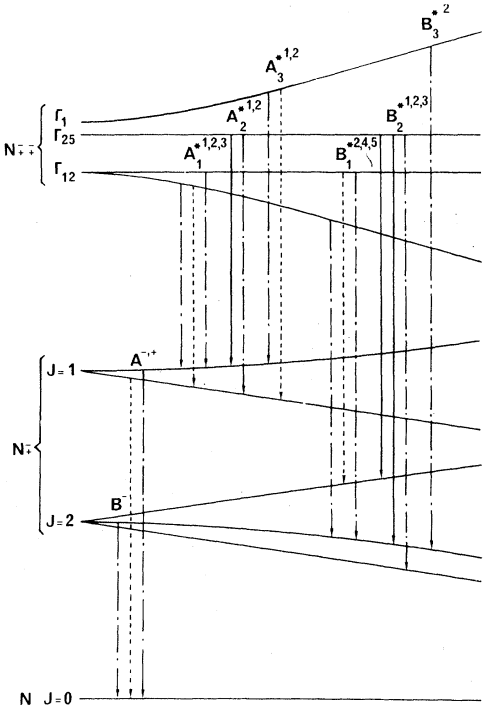


FIG. 2. Shift and splitting of the bound excitonic molecule and bound exciton states under [001] stress. The center-of-gravity shifts have not been included in the figure; they will correspond to additional components $A_1$ for the BE and $A_2$ for each exciton of the BEM. The dipole-allowed transitions are indicated by arrows for $\sigma$ polarization (dot-dashed lines), $\pi$ polarization (dotted lines), and both polarizations (full lines). In this stress configuration the $\Gamma_1$ and $\Gamma_{12}^b$ BEM states are stress coupled, and the $B_3^*$ component becomes stress allowed.

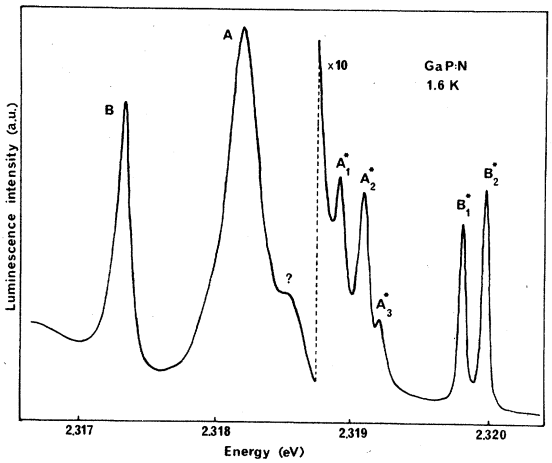


FIG. 3. Typical photoluminescence spectrum obtained at 1.6 K on N-doped GaP samples. The recombination lines are labeled in agreement with the theoretical model given in Sec. II. $A$ and $B$ correspond to the radiative decay of the bound exciton. $A_i^*$ and $B_j^*$ correspond to the radiative decay of one of the two excitons of the bound excitonic molecule. The structure labeled "?" is discussed in the text.

identified. It is possible that this line arises from the decay of a complex consisting of two electrons and one hole bound to an isolated nitrogen. This complex labeled $N^{\mp -}$ is intermediate between the bound exciton ($N^{\mp}$) and the bound excitonic molecule ($N^{\mp\mp}$), and is identical to the ($D^0X$) complex already observed in GaP:S.[16] In this model the two electrons combine with antiparallel spins to form a state $J_e=0$; next the $j=\frac{3}{2}$ hole is repelled and combines with the $J_e=0$ state to form the state $J=\frac{3}{2}$. In the final state of the optical transition, there remains only a single electron of spin $\frac{1}{2}$ bound to N. Thus the model predicts a single line in the optical decay of the $N^{\mp -}$ complex. This corresponds to the experimental result. Moreover, considering Allen's[8] view that the isolated nitrogen impurity cannot bind an electron by itself, the final state of the transition must have a very short lifetime, and consequently the recombination line must be relatively wide; this also corresponds to the observed structure. Now, studies of the stress dependence or Zeeman splitting of this line will provide the only conclusive experimental evidence with respect to the angular momentum assignment. However, these measurements which should be undertaken are very difficult because of the fact that the line is weak and is very close to the strong $A$ component.

### B. Stress dependence

In a preceding paper,[6] we have investigated the effect of uniaxial compressions up to about 8 kbars on the zero-phonon luminescence and absorption spectra associated with the bound exciton: $A$ and $B$ lines. The stress behavior of the BE states was found to be consistent with the $j$-$j$ coupling scheme and very well accounted for by Eq. (8). In particular we have found that the matrix element $\Delta_1$ which characterizes the strength of the intervalley mixing for the BE has a value $\Delta_1=8$ meV.

Now the luminescence lines associated with the BEM ($A^*$ and $B^*$) are clearly observed only under very low-stress conditions, typically up to about 400 bars. On the other hand, it is to be noted that the energy of the luminescence lines is a function of the stress produced near the sample surface. As a consequence, since it is very difficult to measure with sufficient accuracy a very small uniaxial surface stress, we have used as a strain gauge the energy of the $|10\rangle$ BE state which is not stress mixed with other $|JM\rangle$ states. The stress dependence of this BE state is given by $W_1^1$ [Eq. (8a)] and corresponds to the low-energy component of the stress-split $A$ line; it has been labeled $A^-$ in Ref. 6.

The effect of a compressive stress on the $A^*$ and $B^*$ manifolds have been measured for stresses applied along the [001], [111], and [110] crystallographic directions. A typical spectrum is shown in Fig. 4. On the low-energy side we observe clearly the stress-induced splitting of the $A$ and $B$ lines associated with the decay of the BE. The stress dependences of the $A^-$, $A^+$, $B^-$, and $B^+$

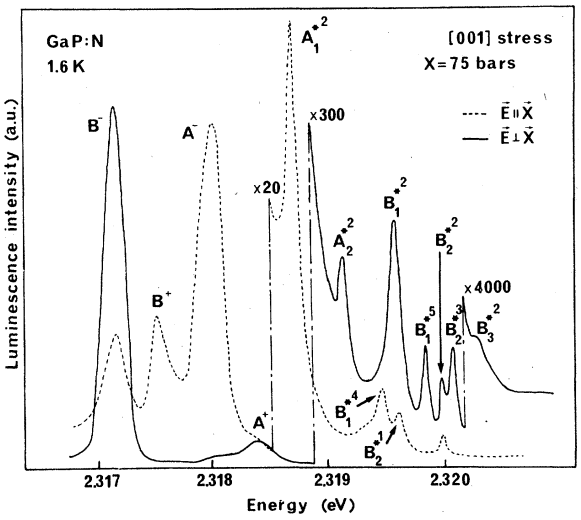


FIG. 4. Typical photoluminescence spectrum obtained at 1.6 K under [001] stress. The various lines are labeled in accordance with the theoretical model given in Sec. II. It should be noted the $B_3^{*2}$ component which is dipole forbidden at zero stress becomes stress allowed in $\sigma$ polarization.

components, which are given by $W_1^1$, $W_1^2$, $W_1^3$, and $W_1^4$ [Eqs. (8a)–(8d)], respectively, have been studied in detail in Ref. 6. From these stress dependences we deduced three other parameters used in the theoretical model given in Sec. II: $a_1 = -0.3$ eV, $\Delta_1 = 8$ meV, and $\epsilon = 1.95$ meV/Kbar.

On the high-energy side we observe nine components of the stress-split $A^*$ and $B^*$ lines. The signal is typically two orders of magnitude lower. The $B_3^{*2}$ component which is dipole forbidden at zero stress becomes stress allowed in $\sigma$ polarization. This very weak component is associated with the higher-energy split state of the BEM (see Fig. 2). Hence, because of the conjugate effects of the stress-induced oscillator strength and of the thermalization, it appears at very low stress and disappears for $X > 100$ bars.

Figures 5, 6, and 7 show the stress splitting of the $A^*$ and $B^*$ lines for stress applied along the [001], [111], and [110] axes, respectively. The full lines ($\sigma$ and $\pi$ polarizations), dashed lines ($\sigma$ polarization) and dotted lines ($\pi$ polarization) correspond to the calculated stress dependences

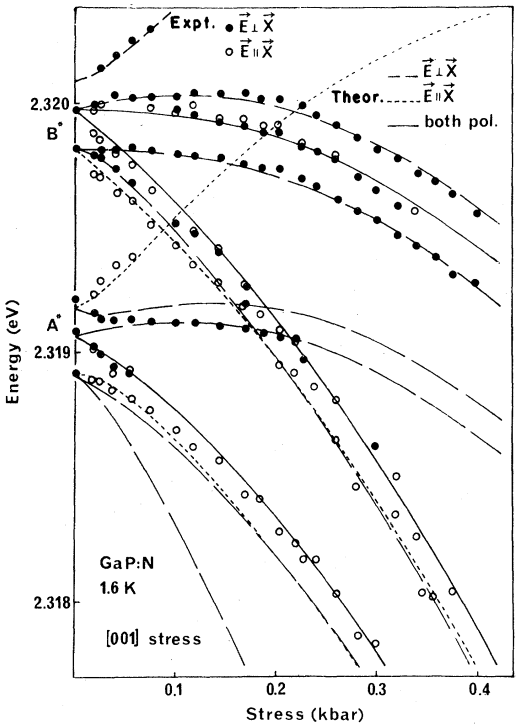


FIG. 5. Stress dependence of the $A^*$ and $B^*$ lines of the excitonic molecules with stress along the [001] crystallographic direction. The data were taken at 1.6 K; solid circles correspond to the $\sigma$ polarization ($E \perp X$), open circles correspond to the $\pi$ polarization ($E \| X$). The full lines (both polarizations), broken lines ($\sigma$ polarization) and dotted lines ($\pi$ polarization) are calculated with Table I and Eqs. (8) and (10). The initial and final states for the transitions shown here are given in Fig. 2. The $B_3^{*2}$ component, which is zero-stress forbidden, appears with increasing stress and disappears at about 100 bars because of thermalization.

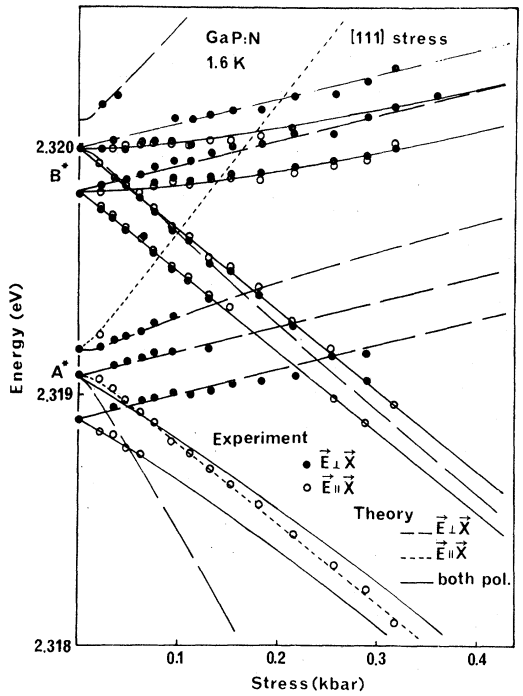


FIG. 6. Same as Fig. 5 with $X \| [111]$.

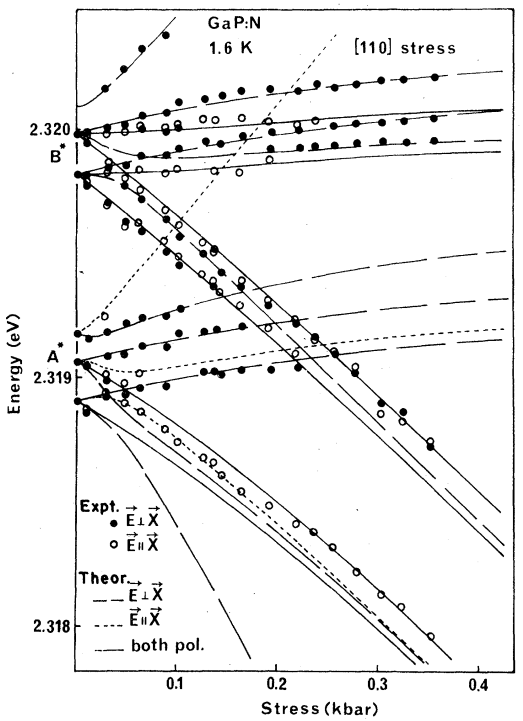


FIG. 7. Same as Fig. 5 with $X \| [110]$.

of the dipole-allowed transitions given in Table I. The values of the different parameters have been obtained either from the zero-stress spectrum ($\gamma = 0.90$ meV, $\delta = 0.18$ meV, $\beta = 0.17$ meV), or from the stress dependences of the BE ($a_1 = -0.3$ eV, $\Delta_1 = 8$ meV, $\epsilon = 1.95$ meV/kbar, $E_2 = 6.9$ eV). The only adjustable parameters are the hydrostatic deformation potential $a_2$ and the intervalley-coupling matrix element $\Delta_2$ of the BEM. The best fit between theory and experiment for all stress directions is obtained by taking $a_2 = 1.33$ eV and $\Delta_2 = 2.3$ meV.

These values are strongly different from the corresponding values quoted for the single bound exciton ($a_1 = -0.3$ eV and $\Delta_1 = 8$ meV). $\Delta_2$ is much smaller than $\Delta_1$ and $a_2$ is closer to the corresponding value for the free exciton (2.3 eV)[15] than is $a_1$. This is in qualitative agreement with the estimate of Merz *et al.*[13] who suggested that in the BEM the two electrons do not occupy the central cell at the same time but that each electron only spends about 10% of its time in the central cell.

The measured value for $\Delta_2$ corresponds to an intervalley splitting $E_{12} = 6.6$ meV and, contrary to the case of the single bound exciton,[6] the $\Gamma_{12}$ valley-orbit split state of the BEM appears now to be a bound state. Until now it has never been observed.

## IV. CONCLUSION

We have investigated the experimental and theoretical stress dependence of the $A^*$ and $B^*$ photoluminescence lines of nitrogen-doped GaP. We have obtained very close agreement between experimental and theoretical shifts for the complex stress behavior. This is strong evidence for the correct identification already reported by Merz *et al.*[13]: $A^*$ and $B^*$ lines result from the radiative recombination of an excitonic molecule bound to a nitrogen atom; the ground states of the transition are the $J = 1$ and $J = 2$ states of the single bound exciton. On the other hand, the intervalley-coupling matrix element $\Delta$ for the bound excitonic molecule appears to be much smaller than the corresponding value for the single bound exciton.

---

*Centre associé au CNRS.

[1]P. J. Dean and D. C. Herbert, in *Excitons*, edited by K. Cho (Springer, New York, 1979), p. 55.
[2]D. G. Thomas, in *Proceedings of the International Conference on the Physics of Semiconductors, Kyoto, 1966*, J. Phys. Soc. Jpn. Suppl. 21, 265 (1966).
[3]P. J. Dean, J Lumin. 12, 398 (1970).
[4]Y. Kenfu, T. Komatsu, and Y. Takimura, J. Phys. Soc. Jpn. 38, 771 (1975).
[5]R. Street and P. J. Wiesner, Phys. Rev. B 14, 632, (1976).
[6]H. Mathieu, L. Bayo, J. Camassel, and P. Merle, Phys. Rev. B 22, 4834 (1980).
[7]R. A. Faulkner, Phys. Rev. 175, 991 (1968).
[8]J. W. Allen, J. Phys. C 1, 1136 (1968); 4, 1936 (1971).
[9]M. Jaros and S. Brand, J. Phys. C 12, 525 (1979) and references therein.
[10]R. A. Faulkner and P. J. Dean, J. Lumin. 1, 552 (1970).
[11]E. Cohen and M. Sturge, Phys. Rev. B 15, 1039 (1977).
[12]J. D. Cuthbert and D. G. Thomas, Phys. Rev. 154, 763 (1967).
[13]J. L. Merz, R. A. Faulkner, and P. J. Dean, Phys. Rev. 188, 1228 (1969).
[14]A. Onton and T. N. Morgan, Phys. Rev. B 1, 2592 (1970).
[15]H. Mathieu, P. Merle, E. L. Ameziane, B. Archilla, J. Camassel, and G. Poiblaud, Phys. Rev. B 19, 2209 (1979).
[16]H. Mathieu, B. Archilla, P. Merle, and J. Camassel, Phys. Rev. B 20, 4268 (1979) and references therein.